Anisotropic damage of concrete: a three-dimensional approach with energy-based loading surfaces and a new evolution law

P. Pröchtel & U. Häußler-Combe
Institute of Concrete Structures, Technische Universität Dresden, Dresden, Germany

ABSTRACT: This paper presents a three-dimensional model to simulate the tensile behavior of concrete based on continuum damage mechanics. By using a symmetric second-order tensor as the damage variable, this model allows for the simulation of orthotropic degradation. Three decoupled loading functions are defined in quantities that are thermodynamically conjugate to the damage variables; the use of these specific definitions yields a symmetric tangent stiffness. In order to allow FE-calculations with arbitrary meshes, a process zone width is introduced in the damage evolution. A Newton-Raphson-Method is used to solve the resulting nonlinear system of equations, and all partial derivatives are presented. Finally, the evaluation of the model is carried out by means of standard experimentation.

1 INTRODUCTION

The tensile behavior of normal concrete beyond its linear elastic range is defined by the formation and growth of microcracks. Over time, concentration and coalescence of these micro defects in a process zone lead to the appearance of macrocracks. By observing the uniaxial, macroscopic behavior, one clearly sees the softening of and a loss of stiffness in concrete as proven by cyclic tensile tests, (Gopalaratnam & Shah 1985). Modelling of these properties can take place by means of continuum damage mechanics, (Lemaitre 1991), (Carol et al. 1994), by applying such concepts as isotropic or anisotropic damage. The anisotropic damage concept should be used for simulating the tensile softening behavior of normal concrete due to the orientation of the resulting load induced microcracks. The realistic simulation of the anisotropy is important, particularly with regard to the computation of reinforced concrete structures, because large compressive stresses must be transferred parallel to the cracks. Anisotropic damage models have been presented, for example, by: (Simo & Ju 1987a); (Simo & Ju 1987b); (Govindjee et al. 1995); (Schmidt-Hurtienne 2000) and (Pölling 2000). Anisotropic damage models are primarily defined by either a strain based or a stress-based loading surface. As shown in section 2.2, a potentially promising approach is the formulation of loading functions in the space of the variables that are thermodynamically conjugate to the damage variables. Such a definition is based on the use of the pseudo-logarithmic damage rate tensor, suggested by (Carol et al. 2001), as the damage variable. This paper presents an orthotropic damage model with three decoupled loading functions, as well as introduces a new damage evolution allowing for FE calculations with arbitrary meshes. Formulating the loading functions in terms of variables that are thermodynamically conjugate to the damage variables requires an iterative method to solve the resulting nonlinear system of equations. This method is explictly described in section 3. In the last section, evaluation of the model is carried out by means of the experiments of (Nooru-Mohamed 1992) and (Winkler 2001).

2 DESCRIPTION OF THE MODEL

2.1 *Damage operator, energy equivalence approach*

The basis of this model is the definition of an effective, intact material, (Carol et al. 2001), (Lemaitre 1991), with an effective stress σ_{ij}^{eff} and an effective strain ϵ_{ij}^{eff}. The derivation of a linear damage operator to connect the effective material state to the nominal material state, described by the nominal stress σ_{ij} and the nominal strain ϵ_{ij}, is the goal of this section. The relationship between these effective quantities is assumed to be linear elastic and isotropic with the stiffness E_{ijkl}^{0}:

$$\sigma_{ij}^{eff} = E_{ijkl}^{0} \epsilon_{kl}^{eff}$$

The constitutive law for the real, damaged material with the damaged stiffness E_{ijkl} and dependent on a

general damage variable D_* is

$$\sigma_{ij} = E_{ijkl}(D_*, E^0_{ijkl})\epsilon_{kl}\,. \tag{1}$$

The variable can be both a scalar and a tensor. The relationship between the nominal and the effective quantities is assumed to be linear. The damage operator is in the form of a fourth order tensor based on the requirement that a second order tensor remain a second order tensor after a linear operation. Utilizing this fact it is then possible to address approaches for stress and strain:

$$\sigma^{eff}_{ij} = A_{ijkl}\sigma_{kl} \quad , \epsilon^{eff}_{ij} = B_{ijkl}\epsilon_{kl} \tag{2}$$

At this point it can only be stated that the operators have the property of minor symmetry since σ_{ij} und ϵ_{ij} are symmetric. In order to proceed with the definition of the damage operator, an equivalence principle must be chosen, (Lemaitre 1991). Therefore, the energy equivalence approach is used. This approach combines the actual material with the effective material based on the assumption that the accumulated elastic energy u is the same in both:

$$\begin{aligned} u = \frac{1}{2}\sigma_{ij}\epsilon_{ij} &= \frac{1}{2}\sigma^{eff}_{ij}\epsilon^{eff}_{ij} \\ &= \frac{1}{2}A_{ijkl}\sigma_{kl}B_{ijrs}\epsilon_{rs} \\ u = \frac{1}{2}(\boldsymbol{\sigma} : \boldsymbol{\epsilon}) &= \frac{1}{2}(\boldsymbol{\sigma} : \mathbf{A}^T) : (\mathbf{B} : \boldsymbol{\epsilon}) \end{aligned} \tag{3}$$

From this, it follows

$$\mathbf{A}^T : \mathbf{B} = \mathbf{I}^4 \quad , \mathbf{B} = \mathbf{A}^{-T} \tag{4}$$

with the fourth order identity tensor $\mathbf{I}^4$. With this the relationship between **A** und **B** is derived by means of the equivalence principle. **A** is chosen as the linear damage operator. Thus, (2) can be written as:

$$\sigma^{eff}_{ij} = A_{ijkl}(D_*)\sigma_{kl}, \quad \epsilon_{ij} = A_{klij}(D_*)\epsilon^{eff}_{kl}$$

$$\epsilon^{eff}_{ij} = \bar{A}_{klij}(D_*)\epsilon_{kl}, \quad \sigma_{ij} = \bar{A}_{ijkl}(D_*)\sigma^{eff}_{kl}$$

whereby the inverse of **A** is labeled as $\bar{\mathbf{A}}$. In order to formulate the operator **A** in detail, a convenient damage variable must be selected. In order to capture the load induced anisotropy of concrete, the use of a second-order symmetric damage tensor D_{ij} is suggested, (Carol et al. 2001) or (Lemaitre 1991). This enables the modeling of orthotropic damage. Matrix representation of the tensor D_{ij} in the principal axes

$$D_{ij} = \begin{bmatrix} D_1 & 0 & 0 \\ 0 & D_2 & 0 \\ 0 & 0 & D_3 \end{bmatrix}$$

allows a comprehensive description of its meaning. The eigenvalues are defined as $0 <= D_k <= 1$ and $k = 1, 2, 3$; whereas, $D_k = 0$ represents intact material and $D_k = 1$ completely destroyed material both in the direction of the eigenvector pertaining to D_k. In the suggested model, however, the integrity tensor $\bar{\phi}_{ij}$ is used

$$\bar{\phi}_{ij} = \delta_{ij} - D_{ij}$$

with the Kronecker delta δ_{ij}. Additionally, the inverse integrity tensor ϕ_{ij} and, for the sake of symmetry, the tensors $\bar{w}_{ij}$ and w_{ij} are introduced, (Carol et al. 2001):

$$\begin{aligned} \bar{\phi}_{ij} = \bar{w}_{ik}\bar{w}_{kj} \quad , \quad \phi_{ij} &= w_{ik}w_{kj} \\ \bar{\phi}_{ik}\phi_{kj} &= \phi_{ik}\bar{\phi}_{kj} = \delta_{ij} \\ \bar{w}_{ik}w_{kj} &= w_{ik}\bar{w}_{kj} = \delta_{ij} \end{aligned}$$

An approach for determing the damage operator **A** in one of these variables is the next step. The formulation used by (Carol et al. 2001) is chosen:

$$A_{ijkl} = \frac{1}{2}(w_{ik}w_{jl} + w_{il}w_{jk})$$

and

$$\bar{A}_{ijkl} = \frac{1}{2}(\bar{w}_{ik}\bar{w}_{jl} + \bar{w}_{il}\bar{w}_{jk}) \tag{5}$$

The nominal, secant constitutive law can be derived by the definition of **A** :

$$\begin{aligned} \sigma_{ij} &= \bar{A}_{ijkl}\sigma^{eff}_{kl} \\ &= \bar{A}_{ijkl}E^0_{klmn}\epsilon^{eff}_{mn} \\ &= \bar{A}_{ijkl}E^0_{klmn}\bar{A}_{opmn}\epsilon_{op} \end{aligned} \tag{6}$$

Substituting (5) yields

$$\sigma_{ij} = \bar{w}_{ip}\bar{w}_{jq}\bar{w}_{kr}\bar{w}_{ls}E^0_{pqrs}\epsilon_{kl} \tag{7}$$

$$\boldsymbol{\sigma} = \mathbf{E}(\mathbf{E}^0, \mathbf{w}) : \boldsymbol{\epsilon} = \mathbf{E}(\mathbf{E}^0, \boldsymbol{\phi}) : \boldsymbol{\epsilon} \tag{8}$$

with the secant stiffness

$$\begin{aligned} E_{ijkl} &= \bar{w}_{ip}\bar{w}_{jq}\bar{w}_{kr}\bar{w}_{ls}E^0_{pqrs} \\ &= \Lambda_0\bar{\boldsymbol{\phi}} \otimes \bar{\boldsymbol{\phi}} + 2G_0\bar{\boldsymbol{\phi}}\,\underline{\overline{\otimes}}\,\bar{\boldsymbol{\phi}} \end{aligned} \tag{9}$$

and the elastic isotropic parameters Λ_0, G_0. The product $\underline{\overline{\otimes}}$ means:
$\mathbf{a}\,\underline{\overline{\otimes}}\,\mathbf{a} = \frac{1}{2}(a_{ik}a_{jl} + a_{il}a_{jk})\mathbf{e}_i \otimes \mathbf{e}_j \otimes \mathbf{e}_k \otimes \mathbf{e}_l$. Finally, a remark on the symmetry of the secant stiffness. Equating (6) with (8) reads

$$E_{ijkl} = \bar{A}_{ijmn}E^0_{mnop}\bar{A}_{klop} \tag{10}$$

and with $E^0_{mnop} = E^0_{opmn}$ the major symmetry of the secant stiffness follows:

$$\begin{aligned} E_{ijkl} &= \bar{A}_{ijmn}E^0_{opmn}\bar{A}_{klop} = \bar{A}_{klop}E^0_{opmn}\bar{A}_{ijmn} \\ &= E_{klij} \end{aligned}$$

2.2 *Evolution rule, principle of maximum energy dissipation*

The goal of this section is the derivation of an evolution rule for the damage, where $\boldsymbol{\phi}$ is the damage variable. With (8), the Helmholtz free energy results for elastic degrading material:

$$\rho_0\psi(\boldsymbol{\epsilon},\mathbf{E}) = \frac{1}{2}\boldsymbol{\epsilon} : \mathbf{E}(\mathbf{E}^0,\boldsymbol{\phi}) : \boldsymbol{\epsilon}$$

The internal variables are $\boldsymbol{\epsilon}$ and $\boldsymbol{\phi}$, and the thermodynamically conjugate variables are $\boldsymbol{\sigma}$ and $\mathbf{Y}_\phi$:

$$\boldsymbol{\sigma} = \rho_0\frac{\partial\psi}{\partial\boldsymbol{\epsilon}} = \mathbf{E} : \boldsymbol{\epsilon} \quad , \mathbf{Y}_\phi = \rho_0\frac{\partial\psi}{\partial\boldsymbol{\phi}}$$

The total differential is

$$\rho_0\dot{\psi} \;=\; \boldsymbol{\epsilon} : \mathbf{E} : \dot{\boldsymbol{\epsilon}} + \rho_0\frac{\partial\psi}{\partial\boldsymbol{\phi}} : \dot{\boldsymbol{\phi}}$$

If this is inserted in the Clausius-Duhem inequality for isothermal processes, then

$$\rho_0\dot{\psi} \leq \boldsymbol{\sigma} : \dot{\boldsymbol{\epsilon}}$$

yields

$$0 \leq [\boldsymbol{\sigma} - \boldsymbol{\epsilon} : \mathbf{E}] : \dot{\boldsymbol{\epsilon}} - \rho_0\frac{\partial\psi}{\partial\boldsymbol{\phi}} : \dot{\boldsymbol{\phi}}$$

whereby the dissipative portion P_{dis} of the process becomes clear as below:

$$P_{dis} = -\rho_0\frac{\partial\psi}{\partial\boldsymbol{\phi}} : \dot{\boldsymbol{\phi}} = -\mathbf{Y}_\phi : \dot{\boldsymbol{\phi}}$$

In order to be able to work with a positive quantity, $-\mathbf{Y}_\phi$ is chosen as the dual variable to $\boldsymbol{\phi}$. At the basis of thermodynamic derivation is the theory of maximized energy dissipation. P_{dis} shall be maximized under the constraints of $\zeta_k = 0, k = 1,2,3$ by means of a Lagrange maximization. The constraints ζ_k are the loading functions F_k that distinguish elastic material response from progressive damage. The basis is the function Ξ with the Lagrange Multipliers $\dot{\lambda}_k$:

$$\Xi \;=\; P_{dis} + \sum_{k=1}^{3}\dot{\lambda}_k\,\zeta_k = -\mathbf{Y}_\phi : \dot{\boldsymbol{\phi}} + \sum_{k=1}^{3}\dot{\lambda}_k\,\zeta_k$$

$$\frac{\partial\Xi}{\partial(-\mathbf{Y}_\phi)} \;=\; 0 \rightarrow$$

$$\dot{\boldsymbol{\phi}} \;=\; \sum_{k=1}^{3}\dot{\lambda}_k\frac{\partial\,\zeta_k}{\partial(-\mathbf{Y}_\phi)} = \sum_{k=1}^{3}\dot{\lambda}_k\frac{\partial\,F_k}{\partial(-\mathbf{Y}_\phi)} \quad (11)$$

Given this, the evolution rule applies for given loading functions F_k. At this point the loading functions F_k are introduced as constraints, however, nothing is known about the variables comprising the loading functions. The following considerations suggest the definition $F_k(-\mathbf{Y}_\phi)$:

- The derivatives $\frac{\partial F_k}{\partial(-\mathbf{Y}_\phi)}$ must exist to calculate the damage evolution $\dot{\boldsymbol{\phi}}$,
- The definition of $F(-\mathbf{Y}_\phi)$ yields a symmetric tangent stiffness, (Carol et al. 1994); this is advantageous.

Furthermore, (11) constrains the freedom of the design of the loading functions. The equation $\dot{\lambda}_k > 0$ is valid for the Lagrange Multipliers. The derivative $\frac{\partial F_k}{\partial(-\mathbf{Y}_\phi)} > 0$ must hold true because it is only possible for damage to increase, which means $\dot{\boldsymbol{\phi}} > 0$. This is valid for all partial derivatives in this case.

2.3 *Pseudo log damage rate*

In the last section the inverse ϕ_{ij} of the integrity tensor was defined as the damage variable and the conjugate quantity $-\mathbf{Y}_\phi$ was suggested to be a variable of the damage surfaces. Utilizing (Carol et al. 2001), $-\mathbf{Y}_\phi = -\rho_0\frac{\partial\psi}{\partial\boldsymbol{\phi}}$ becomes

$$-\mathbf{Y}_\phi = -Y^\phi_{pq} = \frac{-\nu^0}{E^0}(\sigma_{kl}\phi_{kl})\sigma_{pq} + \frac{1+\nu^0}{E^0}\sigma_{pk}\phi_{kl}\sigma_{lq}$$

with the Young's modulus E^0 and Poisson's ratio ν^0 of the intact, isotropic material. A physical meaning of $-Y^\phi_{pq}$ is, however, difficult to recognize and for this reason a definition of $F(-Y^\phi_{pq})$ is disadvantageous. Hence, the "pseudo-logarithmic damage tensor rate "

$$\dot{L}_{rs} = 2\bar{w}_{rp}\dot{\phi}_{pq}\bar{w}_{rs} \quad (12)$$

is introduced as a modified damage variable in (Carol et al. 2001) that is only defined as a rate tensor, in general. The advantage is found in the dual quantity to $\dot{L}_{ij}$, which is a simple and physically comprehensive quantity by which the loading surface is defined:

$$-Y_{ik} = \frac{1}{2}\sigma^{eff}_{ij}\epsilon^{eff}_{jk}$$

Refer to (Carol et al. 2001) for the detailed derivation of $-Y_{ik}$. For example, the first invariant of $-Y_{ik}$ is the stored elastic energy. Transformation of $-Y_{ik}$ into the principal axes yields the stored effective, elastic energy $-Y_\alpha$ in the principal directions $\mathbf{d}^\alpha$. The dissipation potential with these quantities, (Carol et al. 2001), is

$$P_{dis} = -Y_{ij}\dot{L}_{ij}\,,$$

and maximization leads to the evolution rule for $\dot{L}_{ij}$:

$$\dot{L}_{ij} = \sum_{k=1}^{3}\dot{\lambda}_k\frac{\partial\,F_k}{(\partial - Y_{ij})} \quad (13)$$

Additionally, (12) must be solved for $\dot{\phi}_{pq}$ for subsequent derivations.

$$\dot{\phi}_{pq} = \frac{1}{2}w_{pr}\dot{L}_{rs}w_{sq} \quad (14)$$

2.4 *Loading surfaces*

A loading function must contain both a loading state descriptive component defined in $-Y_{ij}$ and a component describing the current material state. Since $\dot{L}_{ij}$ is only defined as a rate tensor, ϕ_{ij} is used as the variable of the second component; this results in a formulation $F_k(-Y_{ij}, \phi_{ij})$ for the loading surfaces. Because this formulation is complicated due to its second-order tensor components, the loading functions are determined in the eigenvalues of $-Y_{ij}$ and ϕ_{ij}. This also enables a simple decoupling, and the proposed structure becomes:

$$F_1(-Y_1, \phi_1)\,, F_2(-Y_2, \phi_2)\,, F_3(-Y_3, \phi_3)$$

Because the subsequent derivations are the same for all three loading surfaces F_k, only the determination of $F_1(-Y_1, \phi_1)$ is demonstrated. Basically, the structure of F_1 is assumed to be

$$F_1(-Y_1, \phi_1) = f_1(-Y_1) - r_1(\phi_1) \tag{15}$$

if the loading portion is $f_1(-Y_1)$ and the material descriptive state is $r_1(\phi_1)$. For this approach, the following material specific assumptions are found:

- Concrete reacts with energy dissipation only on tensile loadings. In this way $f_1(-Y_1)$ becomes $f_1(-\hat{Y}_1)$ with

  $$-\hat{Y}_1 = \frac{1}{2}\left\langle \sigma_1^{eff} \right\rangle \left\langle \epsilon_1^{eff} \right\rangle$$

  and the Mac Auley brackets $\langle .. \rangle$.

- In the uniaxial case concrete has the ability to store added elastic energy up to a value of $u_t = \frac{1}{2}\frac{f_t^2}{E^0}$, with the mean tensile strength f_t. Once the value of u_t is exceeded the concrete responds by dissipating a portion of the additional energy through the formation of crack surfaces. In the uniaxial tension case $-\hat{Y}_1 = \frac{1}{2}\frac{f_t^2}{E^0}$ is valid at the elastic boundary whereby the following form of $f(-\hat{Y}_1)$ is suitable:

  $$f_1(-\hat{Y}_1) = -\hat{Y}_1$$

Based on these assumptions, (15) becomes

$$F_1(-\hat{Y}_1, \phi_1) = -\hat{Y}_1 - r_1(\phi_1) \tag{16}$$

The derivation of a damage evolution $r_1(\phi_1)$ is the next step. This approach is based on the requirement that the actual physical behavior of normal concrete be simulated in uniaxial tension; in particular, the fracture energy G_F must be accurate. It is valid for the uniaxial tensile case

$$\sigma_1^{eff} = \sigma_1 \phi_1\,, \quad \epsilon_1^{eff} = \frac{\epsilon_1}{\phi_1}$$

and in the case of progressive damage the loading funtion is:

$$F_1 = -\hat{Y}_1 - r(\phi_1) = \frac{1}{2}\sigma_1\epsilon_1 - r_1(\phi_1) = 0 \tag{17}$$

Now an approach for $\sigma_1(\epsilon_1)$ is formulated for σ_1 in (17) that models the tensile behavior of normal concrete. The first step is a modification of the stress-crack opening relationship after (Gopalaratnam & Shah 1985):

$$\sigma_1 = f_t e^{-kw} \tag{18}$$

with the crack opening w in $[m]$ and a parameter k. Assuming a maximimum crack opening of $w_c = 0.15mm$, at which point stress can no longer be transferred enables the determination of k for given fracture energy G_F and tensile strength f_t.

$$G_f = \int_0^{w_c} \sigma_1 dw = \int_o^{w_c} f_t e^{-kw} dw$$

In order to obtain a stress-strain law, the crack opening w must be related to a process zone width h, which corresponds in FE-calculations to the element size in the damage direction.

$$\sigma_1 = f_t e^{-k\epsilon_1 \cdot h}$$

Furthermore, taking into account the fact that softening is not supposed to begin before the tensile strength is reached yields:

$$\sigma_1 = f_t e^{-k(\epsilon_1 - f_t/E_0)\cdot h} \tag{19}$$

With this, the relationship $\sigma_1(\epsilon_1)$ for (17) is given. Applying the uniaxial tensile conditions to (7) results in:

$$\sigma_1 = \frac{E_0}{\phi_1^2}\epsilon_1 \tag{20}$$

Comparing (20) with (19) and solving for ϵ_1 provides

$$\epsilon_1(\phi_1) = \frac{1}{k\,h} W\left(\frac{k\,h\,f_t\,\phi_1^2 e^{\frac{k\,h\,f_t}{E_0}}}{E_0}\right)$$

using the Lambert function $W(..)$. Inserting $\epsilon_1(\phi_1)$ into (19) yields an expression $\sigma_1(\phi_1)$. To obtain the formulation of the damage evolution $r_1(\phi_1)$, the expressions $\epsilon_1(\phi_1)$ and $\sigma_1(\phi_1)$ need only be employed in (17). This provides the damage evolution

$$r_1(\phi_1) = \frac{1}{2}\sigma_1(\phi_1)\,\epsilon_1(\phi_1) = \frac{0.5}{k\,h} V_1 f_t e^{(-k(\frac{1}{k\,h}V_1 - \frac{f_t}{E_0})h)}$$

with $Z = e^{(\frac{k\,h\,f_t}{E_0})}$ and $V_1 = W(\frac{k\,h\,f_t\,\phi_1^2 Z}{E_0})$. Inserting $r_1(\phi_1)$ into (16) and parallel procedures for the surfaces F_2 and F_3 yield the three sought-after loading functions:

$$F_k(-\hat{Y}_k, \phi_k) = -\hat{Y}_k - \frac{0.5}{k\,h} V_k f_t e^{(-k(\frac{1}{k\,h}V_k - \frac{f_t}{E_0})h)} \tag{21}$$

3 ALGORITHM

3.1 *System of constitutive equations*

A system of constitutive equations can be developed that can be solved conveniently by using the equations of the last section. The introduction of (13) in (14) yields the evolution rule of ϕ_{ij}

$$\begin{aligned}\dot{\phi}_{pq} &= \frac{1}{2} w_{pr} \sum_{k=1}^{3} \dot{\lambda}_k \frac{\partial F_k}{\partial(-Y_{rs})} w_{sq} \\ &= \frac{1}{2} w_{pr} (\dot{\lambda}_1 N_{rs}^1 + \dot{\lambda}_2 N_{rs}^2 + \dot{\lambda}_3 N_{rs}^3) w_{sq}\end{aligned}$$

with the abbreviation $N_{rs}^k = \frac{\partial F_k}{\partial(-Y_{rs})}$. Adding the equations (8) and (21) completes the system of constitutive equations. Using an implicit Euler scheme leads to

$$\begin{aligned}R_\sigma = 0 &= -\boldsymbol{\sigma}_{n+1} + \mathbf{E}_{n+1}(\boldsymbol{\phi}_{n+1}) : \boldsymbol{\epsilon}_{n+1} \\ R_{F1} = 0 &= (-\hat{Y}_1)_{n+1} - r_1((\phi_1)_{n+1}) \\ R_{F2} = 0 &= (-\hat{Y}_2)_{n+1} - r_2((\phi_2)_{n+1}) \\ R_{F3} = 0 &= (-\hat{Y}_3)_{n+1} - r_3((\phi_3)_{n+1}) \\ R_\phi = 0 &= -\boldsymbol{\phi}_{n+1} + \boldsymbol{\phi}_n + \frac{1}{2} \mathbf{w}_{n+1} \cdot \mathbf{NN} \cdot \mathbf{w}_{n+1}\end{aligned}$$

with $n+1$ defined as current time and n defined as the previous point in time. Furthermore, the abbreviation $\mathbf{NN} = (\Delta\lambda_1 \mathbf{N}^1 + \Delta\lambda_2 \mathbf{N}^2 + \Delta\lambda_3 \mathbf{N}^3)$ is introduced. The unknown variables in the system of constitutive equations are $\boldsymbol{\sigma}_{n+1}, \boldsymbol{\phi}_{n+1}$ and $\Delta\lambda$, and $\boldsymbol{\epsilon}_{n+1}$ is considered as a paramter. In the interest of simplification and clarity, time indices will no longer be included unless absolutely necessary. The system of equations is solved by a Newton-Raphson-Method:

$$\begin{aligned}\boldsymbol{\Phi}^i \delta\mathbf{p}^{i+1} &= -\mathbf{R}^i \\ \mathbf{p}^{i+1} &= \mathbf{p}^i + \delta\mathbf{p}^{i+1}\end{aligned}$$

with

$$\boldsymbol{\Phi} = \begin{bmatrix} \frac{\partial R_\sigma}{\partial \boldsymbol{\sigma}} & \frac{\partial R_\sigma}{\partial \boldsymbol{\phi}} & \frac{\partial R_\sigma}{\partial \lambda_1} & \frac{\partial R_\sigma}{\partial \lambda_2} & \frac{\partial R_\sigma}{\partial \lambda_3} \\ \frac{\partial R_{F1}}{\partial \boldsymbol{\sigma}} & \frac{\partial R_{F1}}{\partial \boldsymbol{\phi}} & \frac{\partial R_{F1}}{\partial \lambda_1} & \frac{\partial R_{F1}}{\partial \lambda_2} & \frac{\partial R_{F1}}{\partial \lambda_3} \\ \frac{\partial R_{F2}}{\partial \boldsymbol{\sigma}} & \frac{\partial R_{F2}}{\partial \boldsymbol{\phi}} & \frac{\partial R_{F2}}{\partial \lambda_1} & \frac{\partial R_{F2}}{\partial \lambda_2} & \frac{\partial R_{F2}}{\partial \lambda_3} \\ \frac{\partial R_{F3}}{\partial \boldsymbol{\sigma}} & \frac{\partial R_{F3}}{\partial \boldsymbol{\phi}} & \frac{\partial R_{F3}}{\partial \lambda_1} & \frac{\partial R_{F3}}{\partial \lambda_2} & \frac{\partial R_{F3}}{\partial \lambda_3} \\ \frac{\partial R_\phi}{\partial \boldsymbol{\sigma}} & \frac{\partial R_\phi}{\partial \boldsymbol{\phi}} & \frac{\partial R_\phi}{\partial \lambda_1} & \frac{\partial R_\phi}{\partial \lambda_2} & \frac{\partial R_\phi}{\partial \lambda_3} \end{bmatrix}$$

$$\mathbf{R} = [\ R_\sigma \quad R_{F1} \quad R_{F2} \quad R_{F3} \quad R_\phi\ ]^T$$

$$\mathbf{p} = [\ \boldsymbol{\sigma} \quad \boldsymbol{\phi} \quad \Delta\lambda_1 \quad \Delta\lambda_2 \quad \Delta\lambda_3\ ]^T$$

The discrete partial derivatives of $\boldsymbol{\Phi}$ are presented in the sections that follow.

3.2 *The partial derivatives of R_σ*

We begin with $\frac{\partial R_\sigma}{\partial \boldsymbol{\sigma}}$:

$$\frac{\partial R_\sigma}{\partial \boldsymbol{\sigma}} = -\mathbf{I}^{4,s} = -\mathbf{I} \underline{\overline{\otimes}} \mathbf{I} = -\frac{1}{2}(\delta_{ik}\delta_{jl} + \delta_{il}\delta_{jk})$$

with the symmetric fourth order identity tensor $\mathbf{I}^{4,s}$, the second order identity tensor $\mathbf{I}$ and the Kronecker delta δ_{ij}. The determination of $\frac{\partial R_\sigma}{\partial \boldsymbol{\phi}}$ is more complicated:

$$\frac{\partial R_\sigma}{\partial \boldsymbol{\phi}} = \frac{\partial \mathbf{E} : \boldsymbol{\epsilon}}{\partial \bar{\boldsymbol{\phi}}} : \frac{\partial \bar{\boldsymbol{\phi}}}{\partial \boldsymbol{\phi}} = (\frac{\partial \mathbf{E}}{\partial \bar{\boldsymbol{\phi}}} : \boldsymbol{\epsilon}) : \frac{\partial \bar{\boldsymbol{\phi}}}{\partial \boldsymbol{\phi}} \tag{22}$$

First, calculating $\frac{\partial \mathbf{E}}{\partial \bar{\boldsymbol{\phi}}}$ by using (9):

$$\frac{\partial \mathbf{E}}{\partial \bar{\boldsymbol{\phi}}} = \Lambda_0(\bar{\boldsymbol{\phi}} \otimes \mathbf{I}^4 + \mathbf{K}^6) + 2G_0(\bar{\boldsymbol{\phi}} \underline{\overline{\otimes}} \mathbf{I}^4 + \frac{1}{2}(\mathbf{R}^6 + \mathbf{S}^6))$$

with $\mathbf{K}^6 = \bar{\phi}_{kl}\delta_{io}\delta_{jp}\mathbf{e}_i \otimes \mathbf{e}_j \otimes \mathbf{e}_k \otimes \mathbf{e}_l \otimes \mathbf{e}_o \otimes \mathbf{e}_p$, $\mathbf{R}^6 = \bar{\phi}_{jl}\delta_{im}\delta_{kn}\mathbf{e}_i \otimes \mathbf{e}_j \otimes \mathbf{e}_k \otimes \mathbf{e}_l \otimes \mathbf{e}_m \otimes \mathbf{e}_n$ and $\mathbf{S}^6 = \bar{\phi}_{jk}\delta_{im}\delta_{ln}\mathbf{e}_i \otimes \mathbf{e}_j \otimes \mathbf{e}_k \otimes \mathbf{e}_l \otimes \mathbf{e}_m \otimes \mathbf{e}_n$.
The right term in (22) is

$$\frac{\partial \bar{\boldsymbol{\phi}}}{\partial \boldsymbol{\phi}} = -\boldsymbol{\phi}^{-1} \underline{\overline{\otimes}} \boldsymbol{\phi}^{-1}$$

The following is valid for the partial derivatives $\frac{\partial R_\sigma}{\partial \lambda_1}, \frac{\partial R_\sigma}{\partial \lambda_2}$ and $\frac{\partial R_\sigma}{\partial \lambda_3}$:

$$\frac{\partial R_\sigma}{\partial \lambda_1} = \frac{\partial R_\sigma}{\partial \lambda_2} = \frac{\partial R_\sigma}{\partial \lambda_3} = 0$$

3.3 *The partial derivatives of R_{F1}, R_{F2} and R_{F3}*

Initially, the process begins with $\frac{\partial R_{F1}}{\partial \boldsymbol{\sigma}}$

$$\frac{\partial R_{F1}}{\partial \boldsymbol{\sigma}} = \frac{\partial f_1}{\partial(-\mathbf{Y})} : \frac{\partial(-\mathbf{Y})}{\partial \boldsymbol{\sigma}^{eff}} : \frac{\partial \boldsymbol{\sigma}^{eff}}{\partial \boldsymbol{\sigma}} \quad . \tag{23}$$

The factors are obtained

$$\begin{aligned}\frac{\partial f_1}{\partial(-\mathbf{Y})} &= \mathbf{t}^1 \otimes \mathbf{t}^1 = \mathbf{N}^1 \\ \frac{\partial(-\mathbf{Y})}{\partial \boldsymbol{\sigma}^{eff}} &= \frac{1}{2}(\mathbf{I} \otimes \boldsymbol{\epsilon}^{eff}) \quad , \frac{\partial \boldsymbol{\sigma}^{eff}}{\partial \boldsymbol{\sigma}} = \mathbf{w} \underline{\overline{\otimes}} \mathbf{w}\end{aligned}$$

using the principal direction $\mathbf{t}^1$ of $-\mathbf{Y}$. The derivatives $\frac{\partial R_{F2}}{\partial \boldsymbol{\sigma}}$ and $\frac{\partial R_{F3}}{\partial \boldsymbol{\sigma}}$ are executed in the same manner. Therefore, they are not presented. Calculating $\frac{\partial R_{F1}}{\partial \boldsymbol{\phi}}$ is the next step:

$$\frac{\partial R_{F1}}{\partial \boldsymbol{\phi}} = \frac{\partial f_1}{\partial \boldsymbol{\phi}} - \frac{\partial r_1}{\partial \boldsymbol{\phi}}$$

For the first term $\frac{\partial f_1}{\partial \boldsymbol{\phi}} = 0$ holds true, and for the second term

$$\frac{\partial r_1}{\partial \boldsymbol{\phi}} = \frac{\partial r_1}{\partial \phi_1} \mathbf{t}^1 \otimes \mathbf{t}^1$$

with the eigenvector $\mathbf{t}^1$ of $\boldsymbol{\phi}$ and

$$\frac{\partial r_1}{\partial \phi_1} = \frac{V_1 \, f_t e^{(-k(\frac{V_1}{k\,h} - \frac{f_t}{E_0})h)}}{k\,h(1+V_1)\phi_1}\,(1-X)$$

with $Z = e^{(\frac{k\,h\,f_t}{E_0})}$ and $V_1 = W(\frac{k\,h\,f_t\,\phi_1^2\,Z}{E_0})$ holds true. Again, the derivatives $\frac{\partial R_{F2}}{\partial \boldsymbol{\phi}}$ and $\frac{\partial R_{F3}}{\partial \boldsymbol{\phi}}$ are calculated in the same manner. Finally, the derivatives $\frac{\partial R_{F1}}{\partial \lambda_1}, \frac{\partial R_{F1}}{\partial \lambda_2}, \frac{\partial R_{F1}}{\partial \lambda_3}, \frac{\partial R_{F2}}{\partial \lambda_1}, \frac{\partial R_{F2}}{\partial \lambda_2}, \frac{\partial R_{F2}}{\partial \lambda_3}, \frac{\partial R_{F3}}{\partial \lambda_1}, \frac{\partial R_{F3}}{\partial \lambda_2}$ and $\frac{\partial R_{F3}}{\partial \lambda_3}$ are all zero.

3.4 *The partial derivatives of R_ϕ*

Finally, the last row of $\boldsymbol{\Phi}$ is calculated. One begins with

$$\frac{\partial R_\phi}{\partial \boldsymbol{\sigma}} = \frac{\partial \frac{1}{2}\Delta\lambda \mathbf{w}\cdot\mathbf{NN}\cdot\mathbf{w}}{\partial \boldsymbol{\sigma}} = 0$$

with $\mathbf{NN} = (\Delta\lambda_1\mathbf{N}^1 + \Delta\lambda_2\mathbf{N}^2 + \Delta\lambda_3\mathbf{N}^3)$.

Next, $\frac{\partial R_\phi}{\partial \boldsymbol{\phi}}$ is calculated as such

$$\begin{aligned}\frac{\partial R_\phi}{\partial \boldsymbol{\phi}} &= -\frac{\partial \boldsymbol{\phi}}{\partial \boldsymbol{\phi}} + \frac{\partial \frac{1}{2}\Delta\lambda \mathbf{w}\cdot\mathbf{NN}\cdot\mathbf{w}}{\partial \boldsymbol{\phi}} \\ &= -\mathbf{I}^{4,s} + \frac{1}{2}\Delta\lambda \frac{\partial \mathbf{A} : \mathbf{NN}}{\partial \boldsymbol{\phi}}\end{aligned}$$

with $\mathbf{A} = \mathbf{w}\,\underline{\overline{\otimes}}\,\mathbf{w}$. Applying the Leibniz-rule, e.g., (Bertram 2005), to the right term yields

$$\frac{1}{2}\Delta\lambda \frac{\partial \mathbf{A} : \mathbf{NN}}{\partial \boldsymbol{\phi}} = \frac{1}{2}\Delta\lambda\left(\frac{\partial \mathbf{A}}{\partial \boldsymbol{\phi}} : \mathbf{NN} + \mathbf{A} : \frac{\partial \mathbf{NN}}{\partial \boldsymbol{\phi}}\right) \quad (24)$$

The partial derivatives $\frac{\partial \mathbf{A}}{\partial \boldsymbol{\phi}}$ and $\frac{\partial \mathbf{NN}}{\partial \boldsymbol{\phi}}$ are:

$$\frac{\partial \mathbf{A}}{\partial \boldsymbol{\phi}} = \frac{\partial \mathbf{A}}{\partial \mathbf{w}} : \frac{\partial \mathbf{w}}{\partial \boldsymbol{\phi}} = \frac{\partial \mathbf{w}\,\underline{\overline{\otimes}}\,\mathbf{w}}{\partial \mathbf{w}} : \frac{\partial \mathbf{w}}{\partial \boldsymbol{\phi}} \quad (25)$$

First the calculation of the left term

$$\frac{\partial \mathbf{w}\,\underline{\overline{\otimes}}\,\mathbf{w}}{\partial \mathbf{w}} = \mathbf{P}^6 + \mathbf{Q}^6 + \mathbf{w}\,\underline{\overline{\otimes}}\,\mathbf{I}^4 \quad (26)$$

with $\mathbf{P}^6 = \frac{1}{2} w_{jl}\delta_{im}\delta_{kn}\mathbf{e}_i \otimes \mathbf{e}_j \otimes \mathbf{e}_k \otimes \mathbf{e}_l \otimes \mathbf{e}_i \otimes \mathbf{e}_m \otimes \mathbf{e}_n, \mathbf{Q}^6 = \frac{1}{2} w_{jk}\delta_{im}\delta_{ln}\mathbf{e}_i \otimes \mathbf{e}_j \otimes \mathbf{e}_k \otimes \mathbf{e}_l \otimes \mathbf{e}_i \otimes \mathbf{e}_m \otimes \mathbf{e}_n$ and then the right side

$$\begin{aligned}\frac{\partial \mathbf{w}}{\partial \boldsymbol{\phi}} = \frac{1}{2\,I_3^w(I_1^w I_2^w - I_3^w)} \big[& I_1^w \boldsymbol{\phi}\,\underline{\overline{\otimes}}\,\boldsymbol{\phi} - (I_1^w)^2(\boldsymbol{\phi}\,\underline{\overline{\otimes}}\,\mathbf{w} + \\ & \mathbf{w}\,\underline{\overline{\otimes}}\,\boldsymbol{\phi}) + (I_1^w I_2^w - I_3^w)(\boldsymbol{\phi}\,\underline{\overline{\otimes}}\,\mathbf{I} + \mathbf{I}\,\underline{\overline{\otimes}}\,\boldsymbol{\phi}) \\ & + ((I_1^w)^3 - I_3^w)\mathbf{w}\,\underline{\overline{\otimes}}\,\mathbf{w} - (I_1^w)^2 I_2^w(\mathbf{w}\,\underline{\overline{\otimes}}\,\mathbf{I} + \mathbf{I}\,\underline{\overline{\otimes}}\,\mathbf{w}) \\ & + ((I_1^w)^3 I_3^w + (I_2^w)(I_1^w I_2^w - I_3^w))\mathbf{I}\,\underline{\overline{\otimes}}\,\mathbf{I}\big]\end{aligned}$$

based on (Rizzi & Carol 2001), with the invariants I_1^w, I_2^w and I_3^w of $\mathbf{w}$. For the chosen loading functions $\frac{\partial \mathbf{NN}}{\partial \boldsymbol{\phi}}$ results in $\frac{\partial \mathbf{NN}}{\partial \boldsymbol{\phi}} = 0$. Finally, $\frac{\partial R_\phi}{\partial \lambda_1}, \frac{\partial R_\phi}{\partial \lambda_2}$ and $\frac{\partial R_\phi}{\partial \lambda_3}$ remain to be determined:

$$\frac{\partial R_\phi}{\partial \lambda_k} = 0.5\mathbf{w}\cdot\Delta\lambda_k\mathbf{N}^k\cdot\mathbf{w}$$

4 BENCHMARKS

This material model was implemented in the FE code being developed at the Institute of Concrete Structures. To verify the model two simulations of plain concrete structures were performed. First the L-shaped-panel test of (Winkler 2001) and subsequently the double-egde notched specimen experiment of (Nooru-Mohamed 1992) were simulated.

4.1 *L-Shaped-Panel*

The geometry with the chosen discretization is shown in Figure 1. The specimen is loaded by displacement u and the corresponding force is labeled with F. The discretization is performed using four node elements in the plane stress case. According to (Winkler 2001), the material properties are $E_0 = 25850N/mm^2, \nu = 0.18$ and $f_t = 2.7N/mm^2$. Given the variation of values for G_f between $65N/m$ and $90N/m$, a calculation was performed at each extreme; $G_f = 65N/m$ and $G_f = 90N/m$. The nonlinear field problem was solved by means of a modified Newton-Raphson-Method. Figure 2 shows the resulting load-displacement curves; the experimental results are indicated in gray. The simulated peak loads are representative of the experimental peak load in particular when $G_f = 65\,N/m$. However, the simulated load-displacement relationship is too stiff. The damage paths of the two simulations are very similar; therefore the path for $G_f = 90N/m$ is given in Figure 3 only. Comparing the experimentally observed crack pattern in Figure 4 with the simulated damage path shows a good correspondence.

4.2 *Double-Egde Notched Specimen*

The geometry of the specimen is shown in Figure 5. Steel plates were attached in order to simulate the load introduction as uniformly as possible. Compared to the experimental setup, additional steel plates were attached at the lower left and upper right sides of the concrete specimen. These plates were necessary due to load introduction problems experienced at the lower left and upper right-hand corners of the concrete specimen. The steel had a high Young's modulus for modeling the much larger dimensions of the steel frame in the experiment. The material parameters of

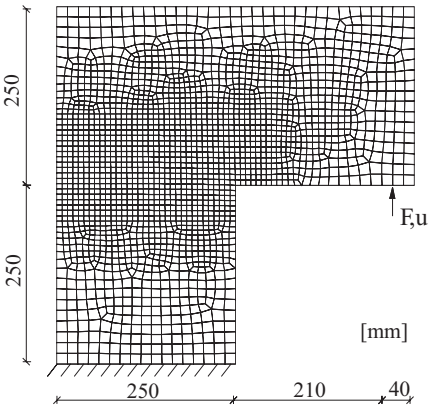

Figure 1: Geometry and discretization of the LSP-experiment

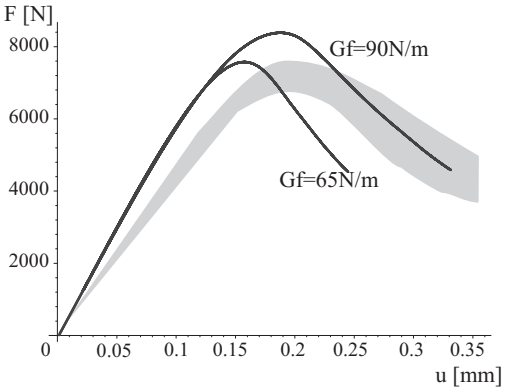

Figure 2: Load-displacement curves

the concrete chosen were $E_0 = 33000\,N/mm^2, \nu = 0.2, f_t = 3.0\,N/mm^2$ and $G_f = 110\,N/m$. The specimen was loaded following load path 4B in (Noorzad-Mohamed 1992). In the first step, the shear load F was applied by being divided into two single loads. In the second step, the force F was held constant while the displacements u were applied. The discretization was performed using four node elements in the plane stress case. The summary of the resulting forces corresponding to prescribed displacements u is labeled with P. Figure 6 shows the resulting load-displacement curves; the experimental results

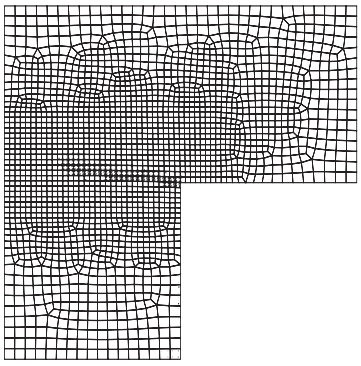

Figure 3: Damage path for $G_f = 90\,N/m$

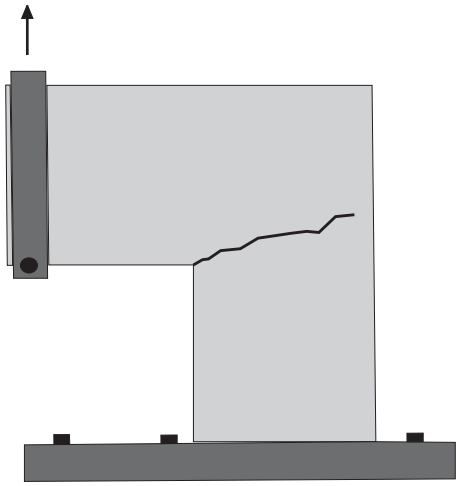

Figure 4: Experimentally observed crack pattern

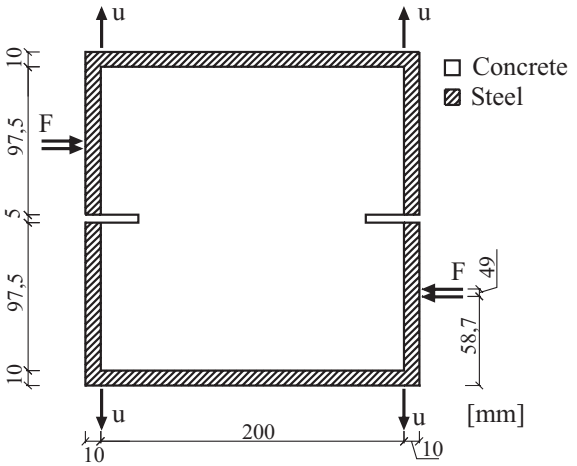

Figure 5: Geometry of the Double Egde Notched Specimen

are shown in gray. The calculated peak load overestimates the experimental result. The damage path is represented in Figure 7 and the experimentally observed crack pattern is shown in Figure 8. The overlapping damaged ranges conform to the experimental macro cracks.

5 CONCLUSIONS

This paper presented an orthotropic model for the tensile behavior of concrete in general three-dimensional

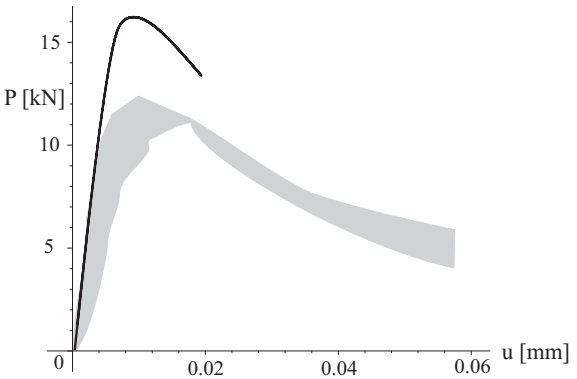

Figure 6: Load-displacement curves

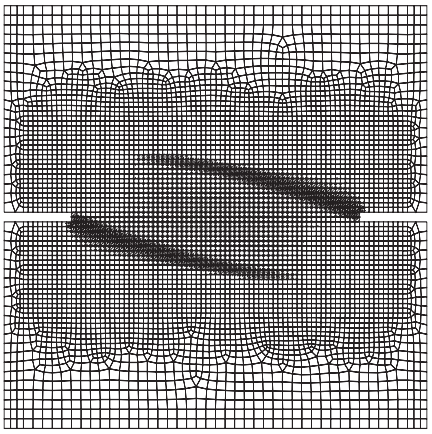

Figure 7: Damage path

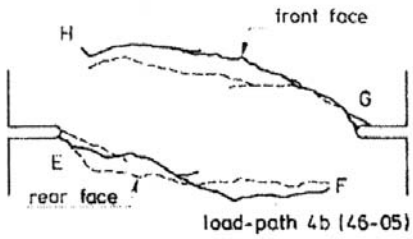

Figure 8: Experimentally observed crack pattern

formulation with the pseudo-log damage rate, suggested by (Carol et al. 2001) as the chosen damage variable. This model contains three decoupled loading functions in which every loading function takes into account one of the three principal directions of the orthotropic damage. This approach simplifies the formulation of the loading functions significantly compared to a coupled formulation. The evolution rule for damage is derived by using the principle of maximum energy dissipation. The introduction of a process zone width allows for the calculation of arbitrary FE discretizations. The calculation of the L-Shaped-Panel test showed a correct peak load and softening behavior. The simulation of the cracked areas was also realistic. The overestimation of the initial stiffnes in Figure 2 may be explained by the fact that the rotational elastic stiffness of the specimen-steel connection was not considered. Calculating the double-edge notched specimen test showed a good simulation of the macrocracks, but the peak load was overestimated. The main difference between the tests of (Nooru-Mohamed 1992) and (Winkler 2001) is the combined mode I and mode II loading in the experiment of Nooru, whereas the specimen in (Winkler 2001) is loaded predominantly as in mode I only. The good results when calculating the tests of Winkler show the capability of the model to simulate mode I loading. However, mixed mode loading showed deficiency of the model. The results of the two simulations give an impression of the capabilities and problems of the proposed model, but, further studies are necessary to correctly evaluate the accuracy of the model and to suggest modifications. Furthermore, the unilateral effect in the behavior of concrete will be included.

REFERENCES

Bertram, A. (2005). *Elasticity and Plasticity of Large Deformations*. Springer.

Carol, I., Rizzi, E. & Willam, K. (1994). A unified theory of elastic degradation and damage based on a loading surface. *International Journal of Solids and Structures 31*(20), 2835–2855.

Carol, I., Rizzi, E. & Willam, K. (2001). On the formulation of anisotropic elastic degradation. I.Theory based on a pseudo logarithmic damage tensor rate. *International Journal of Solids and Structures 4*(38), 491–518.

Gopalaratnam, V. & Shah, S. P. (1985). Softening response of plain concrete in direct tension. *ACI Journal 82*(3), 311–323.

Govindjee, S., Kay, G. J. & Simo, J. C. (1995). Anisotropic modelling and numerical simulation of brittle damage in concrete. *International Journal for Numerical Methods in Engineering 38*(21), 3611–3633.

Lemaitre, J. (1991). *A Course on Damage Mechanics*. Springer.

Nooru-Mohamed, M. (1992). *Mixed-mode fracture of concrete*. Ph. D. thesis, Delft University of Technology.

Pölling, R. (2000). *Eine praxisnahe, schädigungsorientierte Materialbeschreibung von Stahlbeton für Strukturanalysen*. Ph. D. thesis, Ruhr-Universität Bochum.

Rizzi, E. & Carol, I. (2001). A formulation of anisotropic elastic damage using compact tensor formalism. *Journal of Elasticity* (64), 85–109.

Schmidt-Hurtienne, B. (2000, Juli). *Ein dreiaxiales Schädigungsmodell für Beton unter Einschluss des Dehnrateneffekts bei Hochgeschwindigkeitsbelastung*. Ph. D. thesis, Universität Karlsruhe.

Simo, J. & Ju, J. (1987a). Strain and stress-based continuum damage models-I.Formulation. *International Jornal of Solids and Structures 23*(7), 821–840.

Simo, J. & Ju, J. (1987b). Strain and stress-based continuum damage models-II.Computational aspects. *International Jornal of Solids and Structures 23*(7), 841–869.

Winkler, B. (2001). *Traglastuntersuchungen von unbewehrten und bewehrten Betonstrukturen*. Ph. D. thesis, University of Innsbruck.

Wriggers, P. (2001). *Nichtlineare Finite-Elemente-Methoden*. Springer.